Applied Network Science

RESEARCH

Open Access

Influence of adaptive coupling points on coalition formation in multi-energy systems

Rico Schrage[1*] and Astrid Nieße[1]

*Correspondence:
rico.schrage@uni-oldenburg.de

[1] Department of Computer Science, Carl von Ossietzky University Oldenburg, Oldenburg, Germany

Abstract

The share and variants of coupling points (CPs) between different energy carrier networks (such as the gas or power grids) are increasing, which results in the necessity of the analysis of so-called multi-energy systems (MES). One approach is to consider the MES as a graph network, in which coupling points are modeled as edges with energy efficiency as weight. On such a network, local coalitions can be formed using multi-agent systems leading to a dynamic graph partitioning, which can be a prerequisite for the efficient decentralized system operation. However, the graph can not be considered static, as the energy units representing CPs can shut down, leading to network decoupling and affecting graph partitions. This paper aims to evaluate the effect of network adaptivity on the dynamics of an exemplary coalition formation approach from a complex network point of view using a case study of a benchmark power network extended to an MES. This study shows: first, the feasibility of complex network modeling of MES as a cyber-physical system; second, how the coalition formation system behaves, how the coupling points impact this system, and how these impact metrics relate to the CP node attributes.

Keywords: Energy application, Multi-energy system, Complex systems, Complex networks, Coalition formation

Introduction

In energy grids, three crucial short- and mid-term developments are observable: an increase of distributed energy resources (DER), especially renewable energy resources (RER), in the power network, an increase of multi-energy system (MES) forming coupling points (e.g., gas turbines) and the ongoing digitalization of the energy systems. Coupling points can connect various energy carrier networks and create the possibility to transfer energy between different networks, leading to more operational flexibility from the power grid point of view, as energy can be stored more manageably in the form of, for example, hydrogen. However, this comes with the disadvantage of introducing new dependencies between the energy systems. Moreover, the two effects are connected; higher shares of renewable resources need increased system flexibility, which can lead to deploying more coupling points to use other energy carrier networks' flexibility (Mancarella 2014).

Further, coupling points create a necessity to evaluate control strategies with regard to the effects on the coupled networks (Shahidehpour et al. 2005; Xu et al. 2017), and the network topology will be less static with many deployed coupling points, as they can be viewed as energy-transforming links between networks, which can shut down on demand. As a result, coupled networks don't only have to operate as a whole but could get decoupled as well.

Coalition formation (CF) approaches can help to cope with the increasing complexity of the coupled networks and the increase of DERs, their generally small sizing, and their attribute to generate energy mainly in a non-controllable (e.g., due to weather dependencies) way. CF can support in different ways, a) reduce the complexity of distributed control systems and b) allow for small weather-dependent DERs to compete with big power plants like coal or gas plants. For example, either Virtual Power Plants (VPP) (Bitsch et al. 2002; Nieße and Sonnenschein 2015), or clusters of microgrids can be formed to create dynamic optimization approaches which can cope with uncertainty, aggregate flexibility, or even execute distributed optimal power flow (OPF) variations (Zhou et al. 2021; Khavari et al. 2020).

Due to the increase of couplings across different energy sectors, grid topologies are more complex and dynamic than ever. Additionally, the physical energy systems get coupled with *information and communication technology* (ICT) to enable communication between the different parts of the network. This leads to the extension of MES to multi-energy cyber-physical systems (ME-CPS) (Azzouzi et al. 2019) or more general cyber-physical energy systems (CPES).

As a result, the overall system and its operation methods gain in complexity. Further, distributed operating systems require a communication topology. Therefore, investigating coupled multi-carrier networks and their informational topologies, which significantly impact the solution quality in distributed optimization (Holly and Nieße 2021), from a complex systems point of view, seems natural.

In this paper, the research focuses on the dynamic coalition formation behavior in CPES while altering the network and its topology. This leads to the following general research questions we will tackle in this paper.

1. How can a CPES be modeled to conduct research from the complex systems point of view?
2. What is the influence of topology adaptations on coalition formation in CPES, and how do the dynamics relate to important graph metrics representing topology properties?

The paper is structured as follows: First, related work regarding coalition dynamics and complex network applications in energy systems is discussed, and the contributions of this paper are highlighted. Then, we introduce our model and strategy foundations. After the simulation setup is described, we present and discuss the results of the case study. Finally, a conclusion is drawn, and ideas for future work are presented.

Related work

Applying complex network theory is common in investigations of the related electrical grid resilience research area. Also, dynamics of coalition formation considering topology adaptations have been considered in more general settings. However, to our best knowledge, this is the first work that researches large-scale multi-energy (cyber-physical) systems using complex network methods focusing on coalition formation behavior.

A basis for the multi-energy topology analysis has been investigated in Li et al. (2021), in which improved edge weights calculations, metrics, and a case study for a small IEEE test network have been conducted. However, the authors don't focus on adaptive CPs, large-scale networks, or cyber-physical topologies.

Furthermore, there are publications about the influence of coupling points in energy systems from a network planning and control perspective. For example, in Sansawatt et al. (2009), the authors consider the integration of micro-CHPs (micro combined heat and power) and their impact on the distribution power grid. In Xu et al. (2017), it is shown that the coupling of the natural gas and power network can cause significant pressure losses, considering multiple operational modes.

Research on the power grid is also conducted from a complex systems point of view. Pagani and Aiello (2013) present a comprehensive overview of complex network power grid research. This review included research on power grids with 30 to 31,400 nodes with a mean of 4800 and a median of 2100 nodes. Further, much research focuses on reliability analysis (Afzal et al. 2020) using metrics like betweenness centrality (Freeman 1977) or a degree distribution. In these area, the network construction is of a great importance. Complex network methods has shown useful especially for designing and analyzing resilient power grids. For example, the Barabási–Albert scale-free network model Barabasi and Albert (1999) has been applied to the North American electric grid (Chassin and Posse 2005). The authors were able to confirm the accuracy of the model in terms of predicted reliability.

Regarding the coalition formation in adaptive topologies of complex networks, Auer et al. (2015) investigate the formation dynamics using a so-called adaptation rate. This rate determines the speed of topology changes and, at the same time, the speed of the coalition formation. A higher adaptation rate leads to fast topology adaptations with low coalition formation speed and vice versa. This behavior is applied to a network over time to investigate the coalition size and degree distribution, determining the influence of the adaptation rate on the network structure. In contrast to our approach, the adaptations of the topology can occur on every node and edge of the network, so there is no general topology the adaptations are applied to.

The authors of Hasan and Raja (2013) study the emergence of multi-agent coalition formation in complex networks, focusing on its dynamics. However, they did not consider the application to agents in a coupled energy infrastructure, and they naturally had another focus regarding the dynamics of the coalition formation approach. In Feng et al. (2020), the authors introduce a coalition formation approach for energy management in local energy communities. For this, the locality of the agents is utilized to build the neighborhood. This type of local coalition formation is not limited to the energy domain and has also been applied in other areas (Sims et al. 2003).

In this paper, we conduct research to find correlations between coalition formation dynamics and graph theoretical attributes in a multi-energy system. That said, the core novelties and contributions provided by this paper are:

1. A CPES model including different coupling points across three different carrier networks for conducting research using complex network theory, and
2. first insights into the relation between topology adaptation and coalition dynamics using a case study of four multi-energy network variants.

System model

To quantify the influence of coupling points on a coalition formation approach in a CPES, a suitable system model, fulfilling the following requirements, is necessary: (1) the model includes a topology definition to calculate theoretical graph metrics, (2) this graph has to represent the actors and their topology in the coupled grids, (3) the distances in the grid have to be included to limit the neighborhood for the CF, (4) the CF should rely, as it can be part of the grid operation, on the most critical grid objective w.r.t the stability of the isolated grid, balancing the demand and supply, and (5) the coalition formation has to be able to react to topology changes due to the shut down of CPs, so we need to define the splitting behavior of a coalition on a topology change.

As we don't focus on the communication technology, we generally assume a perfect communication infrastructure. Further, all actors know their local physical states and neighborhood perfectly.

The system model is described in four different parts. First, the graph network construction and formalization are presented. Second, the node neighborhood is defined, including the weighting of the edges. Third, we introduce the exemplary coalition formation method and model. Moreover, the systems adaptivity model and the subsequent coalition split strategies are explained.

Network graph

This section presents the methodical approach for defining the network topology using a multi-energy network.

We consider a CPES topology as directed weighted multigraph $G = (V, E)$ with $e = (u, v, j, \psi, \omega) \in E$, $u, v \in V$ with $V \subset \mathbb{N} \times \mathbb{N}$. An edge e is a directed link between two nodes u and v. The characteristic ψ describes the edge type, ω is the edge weight, and j is the edge id to enable multiple edges between two nodes. A node $u = (\kappa, \beta)$ is a pair of natural numbers. The first is an identifier of an actual network unit, and the second identifies the energy carrier network to which it belongs. A coupling point can be modeled as two nodes with different network affiliations and a directed edge between them. Every producing or consuming energy unit will be represented by a node. Nodes are connected if there is a direct physical connection (a pipe, line,...). If two nodes $u, v \in V$ are in the same energy carrier network, there are two edges (u, v, ω, ψ) and (v, u, ω, ψ). Between nodes of different networks, there exists exactly one direction, depending on the type of the coupling point, represented by ψ. As this graph represents the communication topology based on the grid topology, buses and junctions are generally not represented by nodes. However, if

it is necessary to maintain the connected graph (e.g., empty buses), a so-called virtual node will be inserted, representing a bus or junction. This model has the advantage that most nodes are directly connected to their relevant neighbors without considering their bus or junction. Also, using edge weights, the physical properties of the network can be included as well.

Neighborhood definition

In this paper, we will require locality for the coalition formation. This will be implemented with the definition of a fixed-size neighborhood for every single node based on the physical losses between their represented units. Consequently, the neighborhood $\mathcal{N}_k(u)$ of a node u is defined as the nearest k connected nodes from u as starting point. Note that the influence of k is neglected in this paper, as the whole coalition formation methodology is assumed to be a constant in the system.

$$\begin{aligned} &\mathcal{N}_k(u) = \{\mu_1(u), \ldots, \mu_k(u)\} \\ &\text{with } d(u, \mu_i(u)) \leq d(u, \mu_j(u)) \text{ for } i < j \in \mathbb{N} \end{aligned} \tag{1}$$

Here, $d(u, v)$ is the distance between two nodes and $\mu_i(u)$ is the ith neighbor of x. The weight ω of an edge $e \in E$ is defined, depending on the carrier network affiliation. It is defined as relative power loss for edges in the power network.

$$\omega_{\text{power}} = \frac{P_{\text{in}} - P_{\text{out}}}{P_{\text{in}}} \tag{2}$$

The power values P are calculated using the steady-state solver pandapower based on the Newton–Raphson method (Thurner et al. 2018). In gas networks, the mass loss will be calculated similarly.

$$\omega_{\text{gas}} = \frac{M_{\text{in}} - M_{\text{out}}}{M_{\text{in}}} \tag{3}$$

The mass flow rates M are calculated using the steady-state solver pandapipes, which is also based on the Newton–Raphson method (Lohmeier et al. 2020). At last, the heat loss calculation will be executed using the heat transfer equations (Baehr and Stephan 1994).

$$\begin{aligned} \omega_{\text{heat}} &= \frac{H_{\text{loss}}}{3600 \cdot H_{\text{all}}} \\ H_{\text{loss}} &= d \cdot \pi \cdot l \cdot \delta_{\text{ambient}} \cdot \alpha \\ \delta_{\text{ambient}} &= \left| T_{\text{ambient}} - \frac{T_{\text{in}} + T_{\text{out}}}{2} \right| \\ H_{\text{all}} &= m \cdot C \cdot \delta_T \\ \delta_T &= |T_{\text{in}} - T_{\text{out}}| \end{aligned} \tag{4}$$

Here, H_{loss} is the heat power loss, H_{all} is the heat power flow through the edge, d is the inner diameter of the pipeline, l denotes the length, δ_{ambient} is the temperature difference between the water inside the pipeline and the ambient temperature outside, and α denotes the heat transfer coefficient for the pipeline insulation. Further T_{ambient} is the ambient temperature, T_{in} and T_{out} are the temperatures at the start and the end of the pipe, m is the volume of water in the pipeline, C is the specific heat capacity, and finally,

δ_T denotes the temperature difference between the starting- and the endpoint of the pipeline.

Coalition formation

As we aim to investigate the effect of dynamic local coalition formation (DLCF), a formation method has to be implemented. However, a minimal method, with a protocol similar to Ramos et al. (2013), will be used in this work for simplicity and purity. Furthermore, this paper is not about the quality of the coalitions and more about the influence of topology adaptations on existing coalitions over time. The approach could easily be transferred to more complex coalition formation methods to examine their dynamics once the versatility of the modeling approach has been shown.

We define a coalition as set $\zeta \subseteq V$. Virtual nodes can not be part of a coalition. The coalition formation used here has two essential attributes: (1) locality, as described in the previous subsections A and B; (2) it is dynamic in the sense that coalitions can adapt to topology changes every time step when the DLCF conditions are fulfilled.

The following paragraph describes the protocol of the formation process in a multi-agent system. Further, a coalition objective is defined.

To implement the protocol, a multi-agent system will be set up. There is an agent a for every *productive* node $u \in V$. A node is *productive* if it represents a unit that transfers energy into or consumes energy from the system. Therefore, e.g., slack nodes, transformers, and compressors are excluded from being represented by an agent for the CF. The agent can observe its unit and knows the consumed and fed amount of energy. As we consider heating, gas, and electric networks, every agent maintains a vector

$$e_a = \begin{pmatrix} b_{\text{heat}} \\ b_{\text{power}} \\ b_{\text{gas}} \end{pmatrix} \tag{5}$$

representing the energy balances of u.

Every time step, every agent a will search its neighborhood for acceptable coalitions. The agent topology is identical to the network G in subsection A. Given that a is part of coalition ζ_a, another coalition ζ is *acceptable* if and only if

$$\begin{aligned} &\mathcal{A}(\zeta, a) > \mathcal{A}(\zeta_a, a) \\ &\text{with } \mathcal{A}(\zeta, a) = -\sigma(e_a) \cdot \left(\sum_{b \in \zeta} e_b + e_a \right) \\ &\text{with } \sigma(x) = \frac{x}{||x||} \end{aligned} \tag{6}$$

$\mathcal{A}$ is the attraction of an agent to a node based on the energy balance contribution of the represented node. If multiple coalitions in the neighborhood are acceptable the coalition with the highest $A(\zeta, a)$ will be picked. After a decision has been made, the coalition determines whether it will accept the request of the agent if and only if $A(\zeta) \leq A(\zeta \cup \{a\})$. If these checks hold, the requesting agent will be part of the coalition.

Systems adaptivity

The fundamental idea is to consider coupling points in a multi-energy network as a volatile edge between different energy carrier networks. Therefore the system has to adapt itself when a coupling point is switched off. We consider an adaptation-rate α, which is the probability of being switched on/off at a given time step. If the coupling point is switched off, the CP nodes and all connected edges are removed from the topology graph. As a result, the CP can no longer be part of any coalition (due to the enforcement of locality) and will no longer be considered a part of the energy flow calculation. If it is switched on, the removal will be reverted, and the CP will create a singleton coalition as a starting point.

We have to define the behavior of any coalition which contains a shut-down CP. Especially as coalitions can contain participants across network borders, the locality property may be violated after the removal of the CP. This can result in the necessity to split the coalition into parts. Two different splitting strategies will be considered.

Disintegrate (DI) On removal of a CP, which is part of coalition ζ, this strategy results in the disintegration of the whole coalition if there is more than one connected subgraph with maximal size in the induced subgraph of ζ. If the coalition disintegrates, every affected agent immediately searches for a new coalition.

Connected components (CC) With this strategy, removing a CP, which is part of coalition ζ, results in splitting the coalition into the connected subgraphs of the induced subgraph ζ with maximal size. If there is precisely one maximal-sized subgraph, nothing happens.

Definition of coalition dynamics

One prerequisite for this study is to define the dynamics of coalition formation. We define the dynamics as the coalition progression over time and the topology's spatial attributes. The coalition progression can be described using the coalition sizes and the member mixture regarding the energy unit type and their network affiliation. We will mainly use three functions to characterize and formally define the dynamics; first, the distribution of the coalition size over time, and second, the distribution of the network carrier affiliation mixtures over time will be used to describe the structure of the coalitions themselves. Third, because the spatial dynamics are relevant, a distribution over the group degree centrality of coalitions will be included. Regarding the spatial attributes, we assume that overall the centrality of the coalition has the most significant influence on the formation behavior, and the exact topological spatial attributes can be neglected. We define the three mentioned density distribution functions, which will form the model of the coalition dynamics.

$$F_{t,\theta}^{\text{size}}(\zeta_{\text{size}}) = |D_s(Z_{t,\theta}, \zeta_{\text{size}})| \tag{7}$$

$$\begin{aligned} F_{t,\theta}^{\text{mix}}(\zeta_{\text{el}}, \zeta_{\text{gas}}, \zeta_{\text{heat}}) = \big(&|D_m(Z_{t,\theta}, \zeta_{\text{el}})|, \\ &|D_m(Z_{t,\theta}, \zeta_{\text{gas}})|, \\ &|D_m(Z_{t,\theta}, \zeta_{\text{heat}})|\big) \\ \text{with } |D_m(Z_{t,\theta}, \zeta_{\text{el}})| + &|D_m(Z_{t,\theta}, \zeta_{\text{gas}})| + |D_m(Z_{t,\theta}, \zeta_{\text{heat}})| = 1 \end{aligned} \tag{8}$$

$$F_{t,\theta}^{\text{dc}}(\zeta_{\text{dc}}) = |D_c(Z_{t,\theta}, \zeta_{\text{dc}})| \tag{9}$$

The index t represents the timestep and θ the used adaptation rate. In Eq. (7), $F^{\text{size}}_{t,\theta}$ is the region size distribution, ζ_{size} represents the size of a coalition, D_s maps from the set of all coalitions $Z_{t,\theta}$ to these coalitions with the size of ζ_{size}. The equation (8) defines the mixture distribution $F^{\text{mix}}_{t,\theta}$. D_m maps to a set of coalitions with the el/gas/heat mixture percentage $\zeta_{\text{el}}/\zeta_{\text{gas}}/\zeta_{\text{heat}}$. The last Eq. (9) represents the centrality distribution $F^{\text{dc}}_{t,\theta}$. Further, D_c maps to the coalitions with the centrality value ζ_{dc}.

To conclude, the coalition dynamics Φ are described as the combination of the Eqs. (7–9).

$$\Phi = \left(\left(F^{\text{size}}_{t,\theta}, F^{\text{mix}}_{t,\theta}, F^{\text{dc}}_{t,\theta}\right)\right)_{t\in T^*,\theta\in\Theta} \quad \text{with } T^* \subset \mathbb{N} \text{ and } \Theta \subset \mathbb{Q} \tag{10}$$

In the equation, T^* denotes the set of steps in time, and Θ is the set of adaptation rates evaluated within the system.

MES model

The multi-energy system uses a steady-state simulation using the Newton-Raphson method to solve the respective heat, power, and gas equations. The coupling points are modeled as connected components in the respective networks. For example, a power-to-gas (P2G) coupling point is represented by a load node in the power network and a source node in the gas network. The CP is controlled using the loads' demand as a reference set point, which will be converted to the appropriate gas volume to be injected with a given pressure. Therefore, the networks' power- and pipeflow are solved independently, respecting the execution of the coupling point models to set the correct node values before the flow calculation.

As there is no sufficient grid data for coupled multi-energy networks, especially with the structure we assume to be important in the future, we will explain how our grid data is generated.

As a basis, power grid data from *simbench* (Meinecke et al. 2020) is used. *Simbench* datasets contain fully featured power grids and appropriate time-series data. It is a benchmark dataset for novel network planning and operation methods. Given an appropriate *simbench* network, the gas and heat networks must be generated. Considering medium to low-voltage networks, it is assumed that every power node could eventually be a heat and gas node. As more households and industries are connected to the power grid relative to the gas or heat network, deployment rates have been chosen. The heat and gas networks are generated along the power network nodes. As a result, we have a heat and gas network with a similar topology but a smaller deployment density ρ^{energy} of productive nodes. Further, after generating these networks, coupling points will be generated using constant coupling point densities ρ^{cp} for every CP-type: P2G, CHP, and P2H (power-to-heat).

As the coupling points mainly convert energy forms into another with constant efficiency, the technical details of these CPs are omitted.

Table 1 Used parameter sets and deployment rates in the evaluation

Parameter	Values
Θ	{0, 0.01, ..., 0.99, 1}
T^*	{1, 2, ..., 95, 96}
$\rho_{\text{heat}}^{\text{energy}}$	{0.5, 1}
$\rho_{\text{gas}}^{\text{energy}}$	{0.4, 0.8}
$\rho_{\text{chp}}^{\text{cp}}$	{0.6, 1}
$\rho_{\text{p2h}}^{\text{cp}}$	{0.3, 0.6}
$\rho_{\text{p2g}}^{\text{cp}}$	{0.5, 1}

Implementation

The steady-state physical simulation is implemented using pandapipes and pandapower (Thurner et al. 2018; Lohmeier et al. 2020). These tools were chosen because they can calculate the steady-state variables necessary for calculating the network weights, and they further provide a possibility to implement coupling points utilizing the control loop. To model the agents, we used *mango-agents*[1] due to its capabilities of first, asynchronous agent execution and communication, and second, its modular programming model, which allows reusing implementations. For further implementation details, look into the published software artifact for the paper.[2]

Evaluation

To evaluate the introduced system, we conduct a case study based on the simbench (Meinecke et al. 2020) network *1-MV-urban–1-no_sw*. The whole network is generated using the algorithms described in the previous section. Further, the simbench demand and generation profiles are used. Time series data from the dataset (Ong and Clark 2014) is used for the heat and gas network.

An agent topology is deployed as described in subsection *A. Network graph*. In every time step, every agent executes the self-organizing coalition formation routine described in subsection *C. Coalition formation* using a neighborhood defined in *B. Neighborhood definition*. Coupling points are toggled in every timestep using the employed adaptation rate (see subsection *D. Systems adaptivity*).

This system is executed with various adaptation and deployment rates. The parameters are shown in Table 1. The adaptation rate step size is 0.01 to increase the sample size as there is by nature a large variance in the system. The deployments are chosen such that various coupling densities can be compared while the shares of coupling points are reasonable.

Although, only some combination of these parameters are used. Regarding the deployment rates, four combinations will be used and named as listed in Table 2. The number of nodes, edges, the average degree, and the number of producers and consumers are listed in Table 3 to characterize these networks.

[1] https://gitlab.com/mango-agents

[2] https://gitlab.com/digitalized-energy-systems/scenarios/cf-cn-mes

Table 2 Named network variants used in the evaluation

Name	Description	$\rho^{\text{energy}}_{\text{heat}}, \rho^{\text{energy}}_{\text{gas}}, \rho^{\text{cp}}_{\text{chp}}, \rho^{\text{cp}}_{\text{p2h}}, \rho^{\text{cp}}_{\text{p2g}}$
sparse	The most sparse variant using a minimal amount of gas- and heat nodes and coupling points of all types	0.5, 0.4, 0.6, 0.3, 0.5
cp-dense	Characterized by a high density of coupling points, but the general node density is equal to the sparse variant	0.5, 0.4, 1.0, 0.6, 1.0
net-dense	Low density of coupling points, but high density of active nodes in all energy carrier networks	1.0, 0.8, 0.6, 0.3, 0.5
full-dense	High coupling point density and high general active node density in all energy carrier networks	1.0, 0.8, 1.0, 0.6, 1.0

Table 3 Attributes of the network variants

Network	#nodes	#edges	Average degree	Producer			Consumer		
				El.	Gas	Heat	El.	Gas	Heat
sparse	396	617	2.45	134	3	27	139	44	26
cp-dense	395	616	2.52	134	2	42	139	48	24
net-dense	508	664	3.21	134	5	103	139	103	45
full-dense	520	690	3.65	134	6	137	139	113	23

Objective

The main objective of the evaluation is to investigate the change of dynamics of the coalition formation due to coupling point adaptivity in the system. Overall we want to answer the following questions:

1. Does the modeling approach supports answering the research question and evaluation questions (RQ1)?
2. What is the effect of the adaptations on the coalition dynamics, and can we relate these to the topology attributes (RQ2)?

   (a) What is the effect of the adaptation on the average coalition size itself?
   (b) What is the effect of the splitting strategy?
   (c) Can we estimate the influence of single coupling points using graph metrics?
   (d) Can we estimate the participation force of single nodes using graph metrics?

Metrics

For the research, we need to define appropriate metrics which are able to answer the research objective. In the following, all non-trivial metrics used in the evaluation are introduced and motivated.

Coupling points impact The impact of a coupling point x on the coalition's formation behavior can be described by the difference of some global metric m with x being active or inactive, respectively. We define the impact as

$$I_m(x) = m_T(x,\ T_{x,\text{active}}) - m_T(x,\ T_{x,\text{inactive}}) \tag{11}$$

Here, $T_{x,\text{active/inactive}}$ is a set of timesteps in which x is active/inactive, m_T calculates the mean of the metric m_T within the timesteps defined by T_x. For example, metric $m_T(x, T)$ could be the average coalition size in the steps T of some coupling point node x.

Node participation force It is also possible to look at the attributes of a node, which enable participation in the coalition formation or the participation in coalitions with certain coalition attributes like mixture or centrality. In the subsequent sections, we will refer to that as *participation force*. It can be measured using averages over the coalition dynamics described in *Definition of coalition dynamics* and the following paragraphs.

Node betweenness centrality Measuring centrality is important in energy systems, as a removed high centrality node can lead to a significant lack of short paths in the system, which also influences the neighborhood functions of the nodes. The betweenness centrality (Freeman 1977) defines centrality via the number of shortest paths passing through a node z. We calculate the shortest path using the edge weights described in *System Model B*, as the line and pipe distances are not able to describe the actual energy distance. Formally it can be defined as follows:

$$c^{\text{node}}_{\text{betweenness}}(z) = \sum_{u,v \in V} \frac{\gamma(u, v \mid z)}{\gamma(u, v)}. \tag{12}$$

here, $\gamma(u, v)$ is the shortest path from u to v while $\gamma(u, v \mid z)$ is the shortest path from u to v passing through z.

Edge betweenness centrality The coupling point itself is described as a link between two or more networks; consequently, we also want to describe the centrality of edges. For this purpose, the edge betweenness centrality will also be used (Brandes 2008).

$$c^{\text{edge}}_{\text{betweenness}}(e) = \sum_{u,v \in V} \frac{\gamma(u, v \mid e)}{\gamma(u, v)} \tag{13}$$

This equation is nearly identical to the node betweenness centrality with the difference that $\gamma(u, v \mid e)$ requires the path to pass through an edge e rather than a node.

Group degree centrality (normalized) A metric to calculate the centrality of a group of nodes is needed to describe a coalition's centrality. For this purpose, the group degree centrality (Everett and Borgatti 1999) seems feasible, as it is fast to calculate and describes the number of connected nodes to the group. It is calculated by dividing the number of connected nodes to a group of nodes (a coalition) ζ by the number of nodes other than ζ.

$$c^{\text{group}}_{\text{degree centrality}}(\zeta) = \frac{\text{degree}(\zeta)}{|V \setminus \zeta|} \tag{14}$$

Closeness vitality The closeness vitality (Brandes 2005) describes the positional attribute of a node for the participation force of single nodes. It is defined for a node v as the change of the sum of distances between all node pairs, which don't include v. Formally it is defined by the authors of Brandes (2005) as

$$c_{\text{vitality}}(v) = I_W(G) - I_W(G \setminus \{v\}). \tag{15}$$

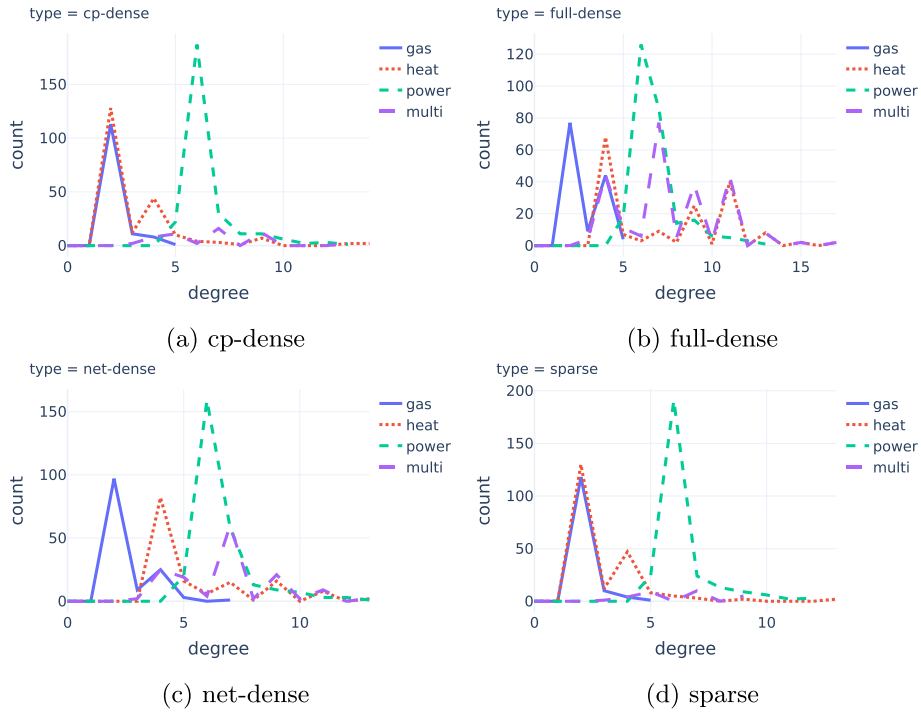

Fig. 1 Degree distribution decomposed by carrier

I_W is the Wiener Index (Wiener 1947) of a graph G. The Wiener Index is the sum of distances between all node pairs.

Results

In this section, we will present the results split into five parts. First, we will introduce the degree distributions of each examined network. Second, the overall system behavior due to the adaptation is shown. Third, we will introduce the evaluation results of the coupling point influence study. Fourth, it is investigated whether graph attributes of single nodes in the network can be used to sense whether and in which types of coalitions the node is included. Finally, the network and its overall node coalition attributes are depicted.

Degree distributions

This study uses four different deployment rate combinations, resulting in four different network variants, shown in Table 2. To show the difference in terms of the degree distribution, Figs. 1 and 2 present the distributions of all network variants, first decomposed by the network without topology changes (Fig. 1a–d), and second combined over all adaptation rates (Fig. 2a, b).

First, the shape of the single distributions can be divided into two different categories, (a) power law distributions and (b) normal distributions. Especially salient, Figs. 1a and d are nearly identical, which makes sense, as the only difference is additional edges in the cp-dense network. Also, net-dense and full-dense distributions look similarly structured, but due to the higher net density, the difference in additional coupling point deployment

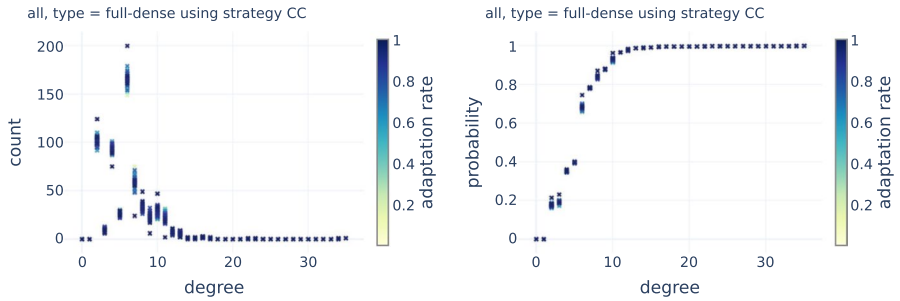

(a) Degree density of the full-dense network (b) Cumulative degree distribution of the full-dense network

Fig. 2 Evaluation of the networks degree distributions over the adaptation rate

is higher in this case. Therefore, from this data, we can predict that the degree distribution may not describe the behavior differences of coalition formation in these network variants.

The combined distribution (not separated by carrier) shown in Fig. 2 reveals that the adaptation rate does not influence the distribution. Further, interpreting the combined distribution can be misleading, as it does not catch the different degree distributions of the single carrier networks.

General behavior of the coalition formation

In this subsection, we want to get a grasp on the influence of the deployment rates (network and coupling point density). In Fig. 3, each network's development of the number of coalitions over time is shown at different adaptation rates. On the left, it is depicted using the DI strategy, and on the right using the CC strategy. It is apparent that the strategy is of major influence. CC generally leads to smoother curves and fewer coalitions over all adaptation rates, time, and network variants. Further, higher adaptation rates lead to more coalitions, and they also increase the influence of the coupling point density. One detail to mention is that the influence of the CP share on the number of coalitions in the simulation with strategy DI is much greater than with using CC. This can be seen when comparing the cp-dense curves in Fig. 3f and e.

To dig deeper into the influence of the adaptation rate on the number of coalitions, Fig. 4 presents the effect of the adaptation rate and the time on the number of regions using the (1,1) network with strategy DI as an example. First, the number of coalitions declines, oscillating slightly over time. Second, the adaptation rate has a nearly linear or slight logarithmic impact on the number of coalitions. Finally, the variance of the impact stabilizes with increasing time, as can be seen in Fig. 4b.

As the last method to describe the system's behavior, the dynamics of coalition dynamics, described in section *Definition of coalition dynamics*, we discuss the distribution and density function regarding the group degree, region size, and mixtures.

The dynamics, shown in Fig. 4d–f, are relatively smooth and similarly distributed. All across these attributes, the adaptation rate influences the distribution smoothly but not linearly. The density function is generally shifted to the left with higher adaptation rates. The distribution of the relative power mixture is depicted as a cumulative distribution

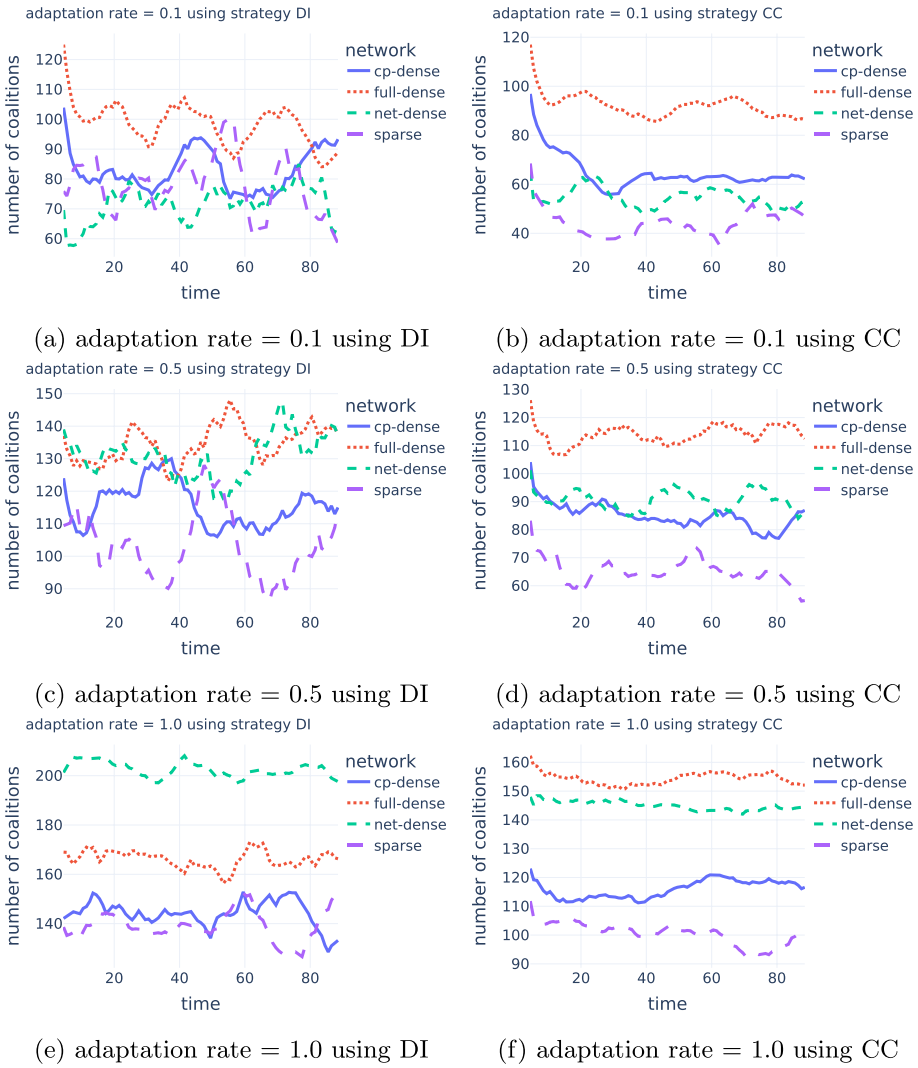

(a) adaptation rate = 0.1 using DI (b) adaptation rate = 0.1 using CC

(c) adaptation rate = 0.5 using DI (d) adaptation rate = 0.5 using CC

(e) adaptation rate = 1.0 using DI (f) adaptation rate = 1.0 using CC

Fig. 3 Number of coalitions over time at different adaptations rate, showing the impact of the deployment rates

function in Fig. 4c. The relative mixture generally considers only mixed coalitions for the sake of visual clarity.

Impact of single coupling points

This subsection presents the impact of single coupling points on the system's behavior. For this, relevant graph metrics, as introduced in the evaluation section, are related to the average impacts of the coupling points over all adaptation rates and timesteps.

First of all, we introduce the methodology of the impact calculation. Figure 5 shows two examples of the raw impact per coupling point (colored and shaped by coupling type). The impact of a CP is defined as the difference between a system metric at times the CP is toggled on and the times it gets toggled off (see the previous "Metrics " section). Figure 5 depicts this impact value over the adaptation rate using two different metrics (average coalition size, left, and heat mixture percentage, right). Regarding the

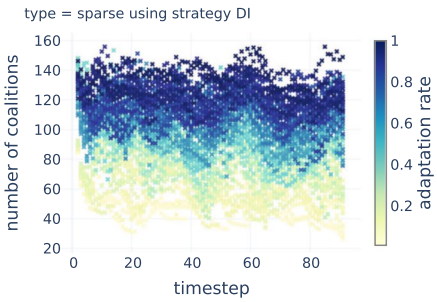

(a) Number of coalitions over time (DI)

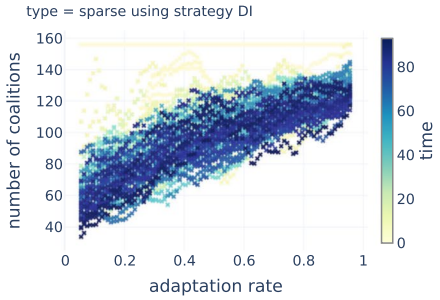

(b) Number of coalitions over time and adaptation rate (DI)

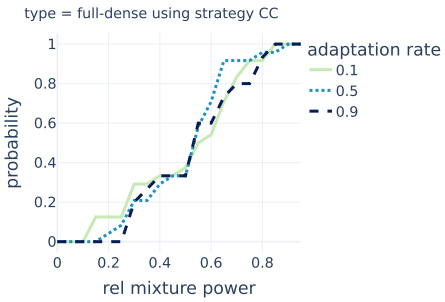

(c) Power mixture distribution by adaptation rate (CC)

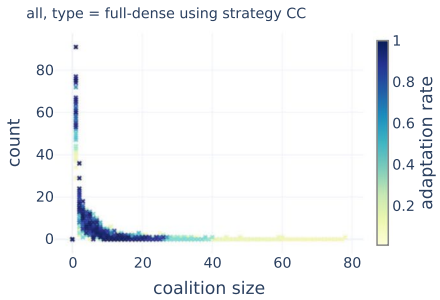

(d) Coalition size distributions by adaptation rate (CC)

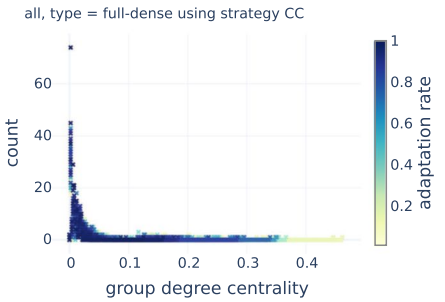

(e) Group degree c. distributions by adaptation rate (CC)

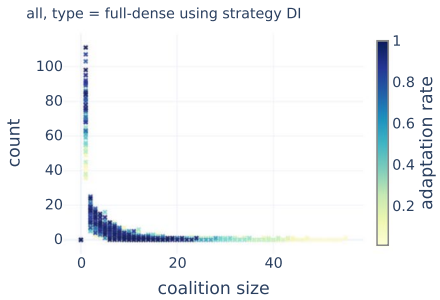

(f) Coalition size distributions by adaptation rate (DI)

Fig. 4 Influence of the adaptation on the system attributes

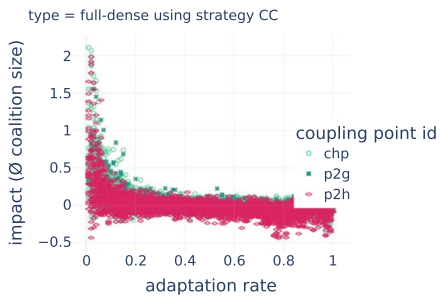

(a) Average size of a coalition over the adaptation rate using CC strategy

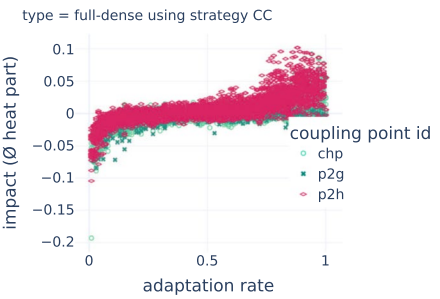

(b) Average heat mixture percentage over the adaptation rate using CC strategy

Fig. 5 Relation between the different impact types of a CP and its static graph attributes

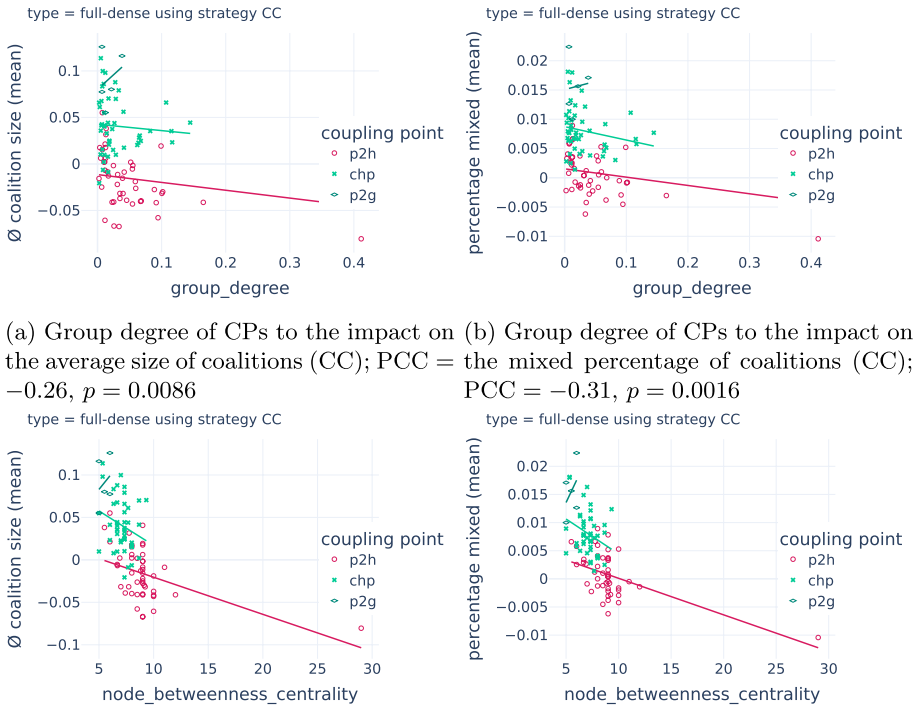

(a) Group degree of CPs to the impact on the average size of coalitions (CC); PCC $= -0.26$, $p = 0.0086$

(b) Group degree of CPs to the impact on the mixed percentage of coalitions (CC); PCC $= -0.31$, $p = 0.0016$

(c) Betweenness centrality of CPs to the impact on the average size of coalitions (CC); PCC $= -0.53$, $p = 1.5 \cdot 10^{-8}$

(d) Betweenness centrality of CPs to the impact on the mixed perc. of coalitions (CC); PCC $= -0.56$, $p = 1.38 \cdot 10^{-9}$

Fig. 6 Relation between graph attributes of CPs and their impact on the coalition formation; including overall Pearson correlation coefficient (PCC) (Pearson 1896) and p-value

average size of a coalition (see Fig. 5a), the CHP and P2G agents appear to have a slightly higher impact overall. However, the impact decreases tremendously with an increase in adaptation. Noting that higher adaptation also equals to stronger side effects from other CPs on the CP impact calculation.

Regarding the heat-node mixture, the impact is negative initially. Following the definition, a negative impact is still a system impact. One could define the impact strength as equal to the impact's absolute value. In this case, the P2H CPs show the highest impact, especially on high adaptation rates.

In the subsequent figures, these impact values are averaged over the adaptation rate for every CP and related to the CP graph metric, as defined in the previous section *Evaluation*.

In Fig. 6, two different metrics were considered, the group degree and the node betweenness centrality of the CP endpoints. Besides these two, the edge betweenness centrality has also been tested, but as it did not show any relation to the impact, the resulting figures are omitted here. Further, only the CC strategy and full-dense network results are shown, as the results for the other parameters are quite similar.

First, the coupling point type dramatically influences the impact, as seen in Fig. 5. Further, with both metrics, group degree in Fig. 6a, b and node betweenness centrality in Fig. 6c, d the coupling point types clusters are distinguishable from each other. Besides, there is a clear relationship between the impact metrics (coalition size and mixed

percentage) and the centrality metrics, especially when looking at the betweenness centrality. The impact of the clusters CHP and P2H is decreasing with increasing centrality, while P2G impact is increasing. Note that the sample size for P2G is way too small for any valuable results. However, when looking at the overall trend of all three clusters combined, the relationship between the impact and the betweenness centrality is clear. To quantify, the Pearson correlation coefficient (Pearson 1896), and the p-value has been calculated (depicted in the captions). In both cases, the absolute coefficient exceeds 0.5 while $p \ll 0.05$, which can be interpreted as a statistically significant moderate linear correlation (although a logarithmic correlation might be more precise due to the definition of the impact). The single trendlines are calculated using the OLS (ordinary least square) procedure.

The result that higher centrality leads to less impact seems counterintuitive. We explain that the less central coupling points might not have an impact on the maximal number of nodes, but it has a more substantial impact, as lower centrality leads, by definition (of the metric and the neighborhood used here), to a smaller set of nodes a node can realistically interact with. As a result, when a CP in such an area of the network is removed, the impact is more severe due to missing fallback alternatives.

Participation force of nodes

In this subsection, we will present the results of the influence of specific nodes and their attributes on the coalitions they participate in. This is referred to as the participation force of a node.

In Fig. 7, the results of this investigation are shown. Like before, only the full-dense network is considered. Further, specifically selected metric combinations are presented. The CC strategy is depicted on the left side of the figure, and the DI strategy is on the right.

The different network clusters are separable in most cases. Overall, all trendlines depict weak relations, primarily with R^2 values smaller than 0.1. The strategies mainly influence the coalition sizes over all network clusters. The participation percentage has a more substantial influence on the heat network than the other two. Generally, the gas network nodes are more resilient to the change in strategies. Strong relations between the nodes' graph attributes and their impact on the coalition formation process are not depicted. The most decisive visible impact would be the network variant; there is a very weak correlation between the node attributes and the coalition metrics of these specific nodes. We can assume that the attribute of a single node is neglectable for its participation in the coalition formation process.

In contrast, the attributes of the coupling points have a clear impact, so the CP distribution and the overall multi-energy system structure are more important for single networks. Furthermore, the attributes of the nodes as part of the energy system have yet to be considered. Therefore, these attributes may dominate the pure graph's theoretical ones.

Graph visualization

To better grasp the fuzzy data obtained in the previous subsection, we continue to investigate the impact of a single node on the coalition formation using a less abstract

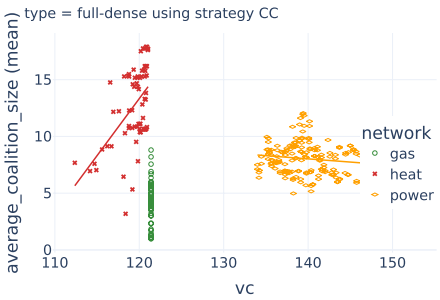

(a) Nodes VC to the mean average coalition size participation of a node (CC)

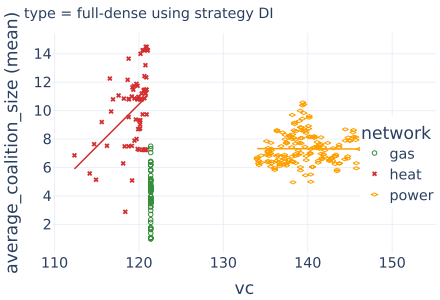

(b) Nodes VC to the mean average coalition size participation of a node (DI)

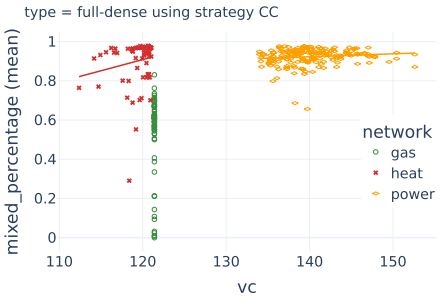

(c) Nodes VC to the mean mixed percentage participation of a node (CC)

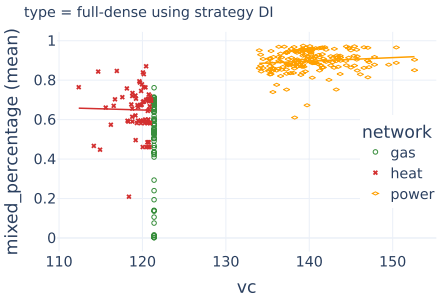

(d) Nodes VC to the mean mixed percentage participation of a node (DI)

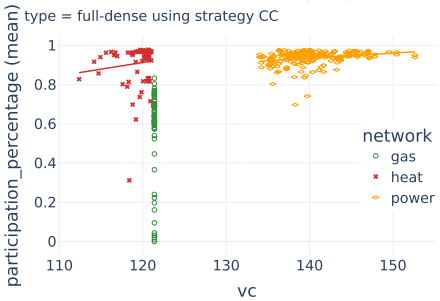

(e) Nodes VC to the mean participation percentage of a node (CC)

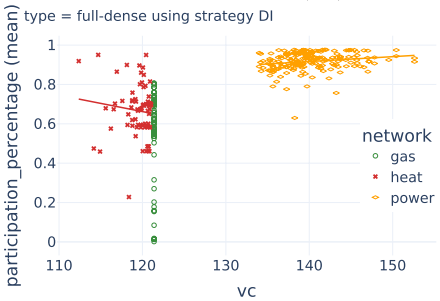

(f) Nodes VC to the mean participation percentage of a node (DI)

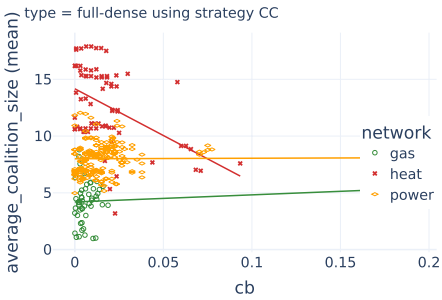

(g) Nodes CB to the mean average coalition size participation of a node (CC)

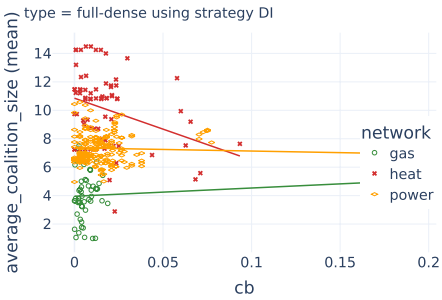

(h) Nodes CB to the mean average coalition size participation of a node (DI)

Fig. 7 Relation between the coalition's participation force at specific nodes and their attributes

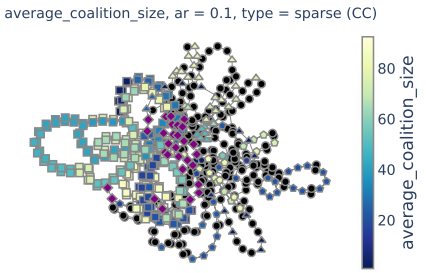

(a) Nodes average coalition size at adaptation rate 0.1

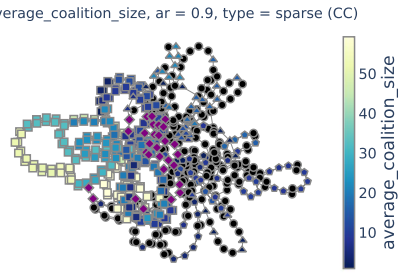

(b) Nodes average coalition size at adaptation rate 0.9

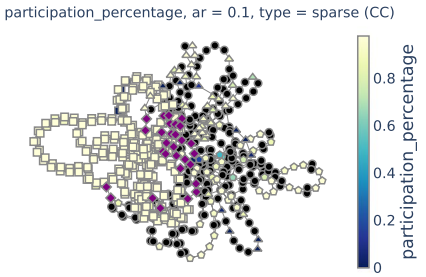

(c) Nodes coalition participation percentage at adaptation rate 0.1

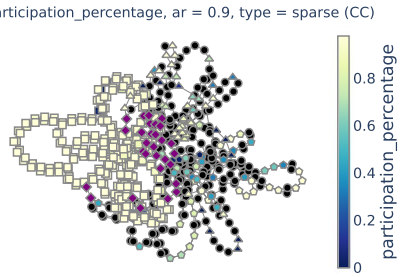

(d) Nodes coalition participation percentage at adaptation rate 0.9

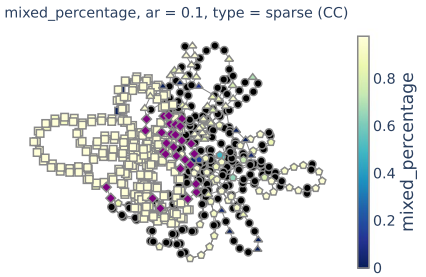

(e) Nodes coalition mixed percentage at adaptation rate 0.1

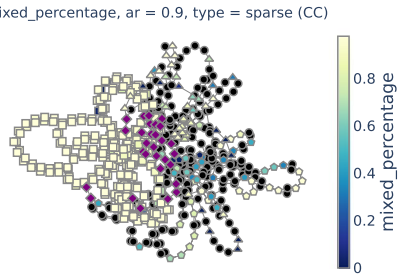

(f) Nodes coalition mixed percentage at adaptation rate 0.9

Fig. 8 Node coalition formation participation statistics in a graph visualization, type: sparse with strategy CC; purple diamonds: coupling points; squares: power nodes; triangles: gas nodes; pentagons: heat nodes

approach. In this subsection, the coalition formation attributes of single attributes are displayed on the complex network itself.

Figure 8 shows the networks, their different types of nodes, and their participation attributes. Three attributes are considered: the average coalition size, participation, and mixed percentage. On the left side of each row, a low adaptation rate (0.1) is depicted, while a high rate (0.9) is on the right. The purple diamond nodes are the coupling points, the black circles are virtual nodes (empty junctions, buses, passive infrastructure nodes), the squares are nodes in the power system, the pentagons are the heating system, and the triangles depict nodes in the gas system. For simplicity, the sparse network with the CC strategy is depicted, layout using the Graphviz (Ellson et al. 2002) library, and its 'neato' (Gansner et al. 2005) graph layout implementation.

The main takeaway from these visualizations is that from the node point of view, centrality/being near coupling points is not the main impact point; it is more relevant to how the neighborhood structure and its attributes look. For example, the leftmost half-circle contains mainly the nodes with high participation and average coalition sizes despite not being as central as some nodes nearer to the coupling points and other networks. This could be because less centrally positioned nodes can be more independent and, therefore, less influenced by the coupling points. Besides, closeness to coupling points might increase the chance of being influenced by higher adaptation rates regarding coalition participation.

Discussion

To conclude the presentation of the results, we will discuss the results with the questions as defined for the evaluation.

What is the effect of the adaptations on the distribution of the coalition size, participant mixture, and centrality metric? The effect on the distribution shape is negligible, looking at a single distribution. However, when taking a view over time, the adaptation leads to a minor oscillating behavior of the coalition formation and, therefore, to the mixture, average size, and coalition centrality. Further, higher adaptation generally results in smaller coalitions strongly influenced by the strategy.

What is the effect of the adaptation on the average coalition size itself? The average coalition size decreases with an increasing adaptation rate.

What is the effect of the splitting strategy? The splitting strategy has two significant impacts: first, it directly influences and strongly affects the coalition sizes, and for the heat network, it leads to smaller participation percentages for some nodes. In general, CC preserves bigger coalitions, while DI leads to smaller coalitions. Second, DI leads to more extreme variance over time. The strategy has a significant impact on coalition formation in adaptive multi-energy systems. These results largely matched our expectations before the experiments were executed.

Can we estimate the influence of single coupling points using graph metrics? In the third subsection of the results, we presented a clear relation between the betweenness centrality and the impact of CPs regarding the coalition size and participation percentage. However, this estimation would not be valid for impact strength.

Can we estimate the participation force of single nodes using graph metrics? The results, described in the fourth and fifth subsections, don't support the existence of a valid relation between the tested graph metrics and the actual participation force. The only usable property for this purpose would be the network as a whole. Further, we could estimate that the placement of the coupling points in the network relate to the participation force itself.

Does the modeling approach support answering the research question and evaluation questions? Analyzing the formation from a complex network perspective with the proposed network model proved feasible for these kinds of analysis, as it abstracts from the complex energy models and network equations in a way that enables us to understand the dynamics and the system's behavior. Furthermore, due to this abstraction, it is also not tied to a specific type of energy network. However, the presented analysis also shows

some limits of this technique. As a result, it might be even more feasible to combine network metrics and energy metrics in the future.

Conclusion

In this work, we first introduced the problem of coalition formation in multi-energy systems and motivated and described its relevance and complexity for MES. Then, an MES modeling approach was presented, feasible to analyze the dynamics of an exemplary supply–demand matching local coalition formations algorithm. This algorithm has been described as a multi-agent system, including a neighborhood definition based on edge weighting in all system parts using estimated losses. Further, an adaptive system was presented in which, as an environment, the influence of the coupling points can be shown. These coupling points introduce one of the main challenges for handling multi-energy systems. To deal with these coupling point adaptations, feasible strategies were presented to handle CP toggling behavior. As a prerequisite for analyzing this system, coalition dynamics in MES were defined, and a technical MES model was introduced to execute the simulation on the adaptive system. The evaluation included a description of the system setup, including system parameters, the used simbench network, and MES data. Further, we defined clear objectives, for which standard metrics were defined to capture and analyze the system behavior. After that, we presented the results of the systems simulation and gave interpretations and explanations of them. At last, the discussion checked whether the evaluation objectives were fulfilled and on which parts other approaches could have been used.

The main finding is that the complex network methods and modeling approach were able to gather valuable information about the MES and the behavior of its coalition formation process. However, it seems limited and needs more specialized hybrid analysis strategies. That could be another way of structuring the network or more energy-related hybrid metrics.

For future work, the next step could be to evaluate the influence of the different parts (objective, protocol, neighborhood definition) of the coalition formation method itself and to include the necessary energy attributes in the conducted research, such as the weights, energy distances, generation and load profile distribution, and node capability distributions. Moreover, success with respect to the coalition formations objective (here, supply–demand matching) can be an essential attribute.

Abbreviations

CPES	Cyber-physical energy system
MES	Multi-energy system
DER	Distributed energy resource
RER	Renewable energy resource
CF	Coalition formation
VPP	Virtual power plant
ME-CPS	Multi-energy cyber-physical system
DLCF	Dynamic local coalition formation
CP	Coupling point
CC	Connected component
DI	Disintegrate
P2G	Power2Gas
CHP	Combined heat power
P2H	Power2Heat
OLS	Ordinary least square

PCC	Pearson correlation coefficient
VC	Vitality closeness
CB	Centrality betweenness

Acknowledgements
Not applicable.

Author contributions
RS came up with the general idea and the implementation and wrote most parts of the manuscript; AN was responsible for supervising, proofreading, and providing ideas for the analysis. All authors read and approved the final manuscript.

Funding
Open Access funding enabled and organized by Projekt DEAL. This work was funded by the DFG (Deutsche Forschungsgemeinschaft) as a part of the DFG SPP 1984.

Availability of data and materials
All cited datasets are publicly available. The source code used for all experiments can be found at https://gitlab.com/digitalized-energy-systems/scenarios/cf-cn-mes. Further, the result data of the experiments are accessible in Schrage (2023).

Declarations

Competing interests
The authors declare that they have no competing interests.

Received: 8 March 2023 Accepted: 22 May 2023
Published online: 02 June 2023

References

Afzal S, Mokhlis H, Illias HA, Mansor NN, Shareef H (2020) State-of-the-art review on power system resilience and assessment techniques. IET Gener Trans Distrib 4(25):6107–6121. https://doi.org/10.1049/iet-gtd.2020.0531
Auer S, Heitzig J, Kornek U, Schöll E, Kurths J (2015) The dynamics of coalition formation on complex networks. Sci Rep. https://doi.org/10.1038/srep13386
Baehr HD, Stephan K (1994) Wärme-und Stoffübertragung, vol 7. Springer, Berlin, pp 34–88
Barabasi A-L, Albert R (1999) Emergence of scaling in random networks. Science 286:509
Bitsch R, Feldmann W, Aumayr G (2002) etz-Jg. Virtuelle kraftwerke-einbindung dezentraler energieerzeugungsanlagen 123:2–9. https://doi.org/10.1186/s42162-018-0033-3
Brandes U (2005) Network analysis: methodological foundations, vol 3418. Springer, Berlin. https://doi.org/10.1007/b106453
Brandes U (2008) On variants of shortest-path betweenness centrality and their generic computation. Soc Netw 30(2):136–145. https://doi.org/10.1016/j.socnet.2007.11.001
Ellson J, Gansner E, Koutsofios L, North SC, Woodhull G (2002) Graphviz—open source graph drawing tools. In: Mutzel P, Jünger M, Leipert S (eds) Graph drawing. Springer, Berlin, pp 483–484
Everett MG, Borgatti SP (1999) The centrality of groups and classes. J Math Sociol 23(3):181–201. https://doi.org/10.1080/0022250X.1999.9990219
Feng C, Wen F, You S, Li Z, Shahnia F, Shahidehpour M (2020) Coalitional game-based transactive energy management in local energy communities. IEEE Trans Power Syst 35(3):1729–1740. https://doi.org/10.1109/TPWRS.2019.2957537
Freeman LC (1977) A set of measures of centrality based on betweenness. Sociometry 40(1):35–41. https://doi.org/10.2307/3033543
Gansner ER, Koren Y, North S (2005) Graph drawing by stress majorization. In: Pach J (ed) Graph drawing. Springer, Berlin, pp 239–250
Khavari F, Badri A, Zangeneh A (2020) Energy management in multi-microgrids considering point of common coupling constraint. Int J Electr Power Energy Syst 115:105465. https://doi.org/10.1016/j.ijepes.2019.105465
Lohmeier D, Cronbach D, Drauz SR, Braun M, Kneiske TM (2020) Pandapipes: an open-source piping grid calculation package for multi-energy grid simulations. Sustainability. https://doi.org/10.3390/su12239899
Mancarella P (2014) MES (multi-energy systems): an overview of concepts and evaluation models. Energy 65:1–17. https://doi.org/10.1016/j.energy.2013.10.041
Meinecke S, Sarajlić D, Drauz SR, Klettke A, Lauven L-P, Rehtanz C, Moser A, Braun M (2020) Simbench–a benchmark dataset of electric power systems to compare innovative solutions based on power flow analysis. Energies 13(12):3290. https://doi.org/10.3390/en13123290
Pagani GA, Aiello M (2013) The power grid as a complex network: a survey. Phys A Stat Mech Appl 392(11):2688–2700. https://doi.org/10.1016/j.physa.2013.01.023
Pearson K (1896) Mathematical contributions to the theory of evolution.–III. Regression, heredity, and panmixia. Philosoph Trans R Soc Lond Ser A 187:253–318
Shahidehpour M, Fu Y, Wiedman T (2005) Impact of natural gas infrastructure on electric power systems. Proc IEEE 93(5):1042–1056. https://doi.org/10.1109/JPROC.2005.847253
Thurner L, Scheidler A, Schäfer F, Menke J, Dollichon J, Meier F, Meinecke S, Braun M (2018) Pandapower–an open-source python tool for convenient modeling, analysis, and optimization of electric power systems. IEEE Trans Power Syst 33(6):6510–6521. https://doi.org/10.1109/TPWRS.2018.2829021

Wiener H (1947) Structural determination of paraffin boiling points. J Am Chem Soc 69(1):17–20. https://doi.org/10.1021/ja01193a005
Zhou B, Zou J, Chung CY, Wang H, Liu N, Voropai N, Xu D (2021) Multi-microgrid energy management systems: architecture, communication, and scheduling strategies. J Mod Power Syst Clean Energy 9(3):463–476. https://doi.org/10.35833/MPCE.2019.000237
Azzouzi E, Jardin A, Bouskela D, Mhenni F, Choley J-Y (2019) A survey on systems engineering methodologies for large multi-energy cyber-physical systems. In: 2019 IEEE international systems conference (SysCon), pp 1–8. https://doi.org/10.1109/SYSCON.2019.8836741
Chassin DP, Posse C (2005) Evaluating North American electric grid reliability using the Barabási–Albert network model 10
Hasan MR, Raja A (2013) Emergence of multiagent coalition by leveraging complex network dynamics. In: Proc. Fifth Int. workshop on emergent intelligence on networked agents, pp 1–15
Holly S, Nieße A (2021) Dynamic communication topologies for distributed heuristics in energy system optimization algorithms, pp 191–200. https://doi.org/10.15439/2021F60
Li J, Song K, He X, Luo H (2021) Reliability evaluation of a regional integrated energy system based on complex network theory. In: 2021 IEEE sustainable power and energy conference (iSPEC), pp 840–845. https://doi.org/10.1109/iSPEC53008.2021.9736060
Nieße A, Sonnenschein M (2015) A fully distributed continuous planning approach for decentralized energy units. In: INFORMATIK 2015
Ong S, Clark N (2014) Commercial and residential hourly load profiles for all TMY3 locations in the United States. https://doi.org/10.25984/1788456
Ramos GdO, Rial JCB, Bazzan ALC (2013) Self-adapting coalition formation among electric vehicles in smart grids. In: 2013 IEEE 7th international conference on self-adaptive and self-organizing systems, pp 11–20. https://doi.org/10.1109/SASO.2013.12
Sansawatt T, Whiteford JRG, Harrison GP (2009) Assessing the impact of micro CHP on gas and electricity distribution networks. In: 2009 44th international universities power engineering conference (UPEC), pp 1–5
Schrage R (2023) Dataset: influence of adaptive coupling points on coalition formation in multi-energy systems: simulation result tables. https://doi.org/10.5281/zenodo.7708253
Sims M, Goldman CV, Lesser V (2003) Self-organization through bottom-up coalition formation. In: Proceedings of the second international joint conference on autonomous agents and multiagent systems, pp 867–874
Xu X, Li K, Jia H, Guo Y (2017) Interactions between gas networks and microgrids through microturbines. In: 2017 IEEE power & energy society general meeting, pp 1–5. https://doi.org/10.1109/PESGM.2017.8274499

Publisher's Note